CORRECTING THE LHC $\beta^\star$ AT COLLISION

W. Wittmer[♣], A. Verdier[◇], F. Zimmermann[◇]
♣ CERN, Geneva, Switzerland and University of Technology Graz, Austria
◇ CERN, Geneva, Switzerland

Abstract

To correct the $\beta^\star$ at the main collision points (IP1 and IP5) simultaneously for the two counterrotating proton beams in the Large Hadron Collider (LHC), a set of specific quadrupoles in the non-common part of the machine is used. Due to the antisymmetric optics, several quadrupoles on each side of the insertion have to be employed. The change of $\beta^\star$ is accomplished by incrementing the quadrupole gradients. This set of increments is referred to as $\beta^\star$ tuning knob. The increments were calculated by rematching $\beta^\star$ in a range of $\pm$ 20 % about the nominal value. Linear curves were fitted to the variation of increments to construct a linear tuning knob. This was done for each plane using MAD 8 [1] and repeated with MAD X [2]. The linear behaviour and the orthogonality of the knobs were investigated for the LHC lattices V6.2 and V6.4. Different field errors were introduced in the lattice and the correction efficiency of the knobs was studied.

1 INTRODUCTION

In LHC operation the beam sizes of the two beams have to be corrected. Two orthogonal knobs can correct each plane independently. To form these knobs, a set of quadrupoles, which are located on each side of the IP in the insertion, are available. From these quadrupoles a knob is constructed so that a specific strength change ΔK is assigned to each, which we refer to as knob vector, so that the $\beta^\star$ is changed. To scale the $\beta^\star$ the knob vector $\Delta \vec{K}$ is multiplied with a variable m which acts as the actual knob. The two knobs should have the following characteristics within a variation of $\pm 20\%$: be orthogonal in the x- and y- plane, create no beta beating in the rest of the ring, scale linearly with $\beta^\star$, not change other constraints (e.g. dispersion, crossing angle), be able to correct the $\beta^\star$ independently of the source of the error and be simple for operation.

The performance of the knobs has to be tested. Therefore, both knobs, when varied over their nominal range, must meet the conditions of the different criteria described above. If this is the case a second stage of testing is started. Various errors are introduced in the lattice and the knobs are used to correct them. This is done step by step to see to which types of errors the knobs can be applied.

2 CALCULATING $\beta^\star$ TUNING KNOBS

The design of the LHC insertion is asymmetric and the beams pass through the inner triplet (Q1–Q3 left and right from the IP) in a common beam pipe off center of the magnetic field axis. Therefore the magnets of the inner triplet cannot be used to correct the effects of errors outside of the triplet, as the two rings are different. The closest magnets that can be used are Q4 left and right of the IP. There are further three quadrupoles upstream (Q5–Q7) which can be used without any restriction. Q8 to Q13 can also be used, but, as part of the dispersion suppressor, not without restriction. Because of the asymmetric β-functions, the different phase advances and the need to correct both planes, there is no single pair of quadrupoles that can do the correction for either of the planes without changing the other plane's β-function. The position of the different tuning quadrupoles and the dipoles separating and combining the two beams is shown in Fig.1.
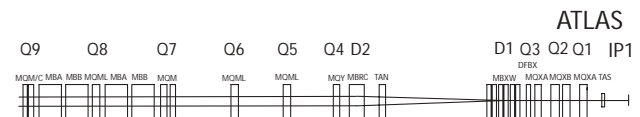

Figure 1: Position of the different magnets on the left side of IR1 and parts of the dispersion suppressor.

Using Q4–Q9 and Q13 scaled to the same relative ΔK as Q9, left and right of the IP, a tuning knob was constructed with MAD8. The version of the lattice file for the LHC was collision optics V6.2. A detailed description of the calculation can be found in [5].

Recently, the crossing angle and other minor changes were re-introduced in the LHC lattice with version V6.4. Also the new version of MAD, MAD X, was defined as the new standard to simulate the LHC lattice. MADX is described in [2]. Therefore, the performance of the knobs had to be reviewed for this new modelling enviroment and compared to earlier results with MAD 8 and V6.2 [5]. The effect of the knobs on the closed orbit in presence of the nominal crossing angle was investigated, in particular the position and slope at the IP.

To distinguish between sources of changes coming either from the change of the lattice or from the crossing angle the characterisation was repeated twice, with crossing angle on and off, respectively. The vertical crossing angle has a negligible influence on the changes of $\Delta\beta_x^\star, \Delta\beta_y^\star, \Delta\alpha_x^\star, \Delta\alpha_y^\star, Q_x, Q_y, D_x^\star, D_y^\star, X^\star, pX^\star$ at the IP as a function of $\Delta\beta_x^\star$ and $\Delta\beta_y^\star$ for a variation of $\pm20\%$. Therefore, only the results with crossing angle on are summarized in Table1. The vertical crossing angle results in a noticable variation of vertical orbit $Y^\star$ and slope $pY^\star$ at the IP.

Table 1: Changes of $\Delta\beta_x^\star$, $\Delta\beta_y^\star$, $\Delta\alpha_x^\star$, $\Delta\alpha_y^\star$, Q_x, Q_y, D_x, Dp_x, $X^\star$, $Y^\star$, $pX^\star$, $pY^\star$ as a function of $\Delta\beta_x^\star$ and $\Delta\beta_y^\star$ for $\pm 20\%$ changes in the presence of a vertical crossing angle ($\pm 150\mu rad$) for V6.4.

VAR	$\beta_x^\star$ $\beta_y^\star$	+20% +20%	+20% −20%	−20% +20%	−20% −20%
$\Delta\beta_x^\star/[\%]$		1.9	1.7	−2.6	−0.5
$\Delta\beta_y^\star/[\%]$		3.7	−3.7	2.4	1.5
$\Delta\alpha_x^\star/[1]$		$4.54E-2$	$1.39E-2$	$2.00E-2$	$5.64E-2$
$\Delta\alpha_y^\star/[1]$		$-4.43E-2$	$-6.73E-2$	$1.22E-2$	$5.43E-2$
$\Delta Q_1/[1]$		−0.009	0.003	−0.001	0.014
$\Delta Q_2/[1]$		−0.009	−0.009	0.009	0.015
$\Delta D_x^\star/[m]$		$2.78E-3$	$3.88E-3$	$-3.40E-3$	$-2.36E-3$
$\Delta D_y^\star/[m]$		$4.19E-4$	$1.66E-4$	$3.29E-4$	$-5.10E-4$
$\Delta X^\star/[m]$		$4.15E-11$	$8.27E-11$	$3.40E-11$	$6.38E-11$
$\Delta Y^\star/[m]$		$2.85E-6$	$2.47E-6$	$-2.30E-6$	$-2.79E-6$
$\Delta pX^\star/[1]$		$1.51E-10$	$1.27E-10$	$1.12E-10$	$2.26E-10$
$\Delta pY^\star/[1]$		$3.91E-6$	$4.61E-6$	$-2.89E-6$	$-5.14E-6$

The responses of $\Delta\beta_x^\star$ and $\Delta\beta_y^\star$ show a slightly degraded behaviour due to the lattice change from version V6.2 to V6.4. The behaviour of $\Delta\beta_y^\star$ is shown in Fig.2.

The changes of $\Delta\alpha_x^\star$, $\Delta\alpha_y^\star$, $\Delta D_x^\star$, $\Delta D^\star$, $\Delta X^\star$, $\Delta pX^\star$, $\Delta pY^\star$, ΔQ_1 and ΔQ_2, are acceptable for adjustments in operation. However, for changes in $\beta_{x,y}^\star$ of $\pm 20\%$ the change of $Y^\star$ (the vertical position at the IP) exceeds $\pm 10\%$ of the nominal beam size as shown in the left plot of Fig. 3. This effect is under investigation.
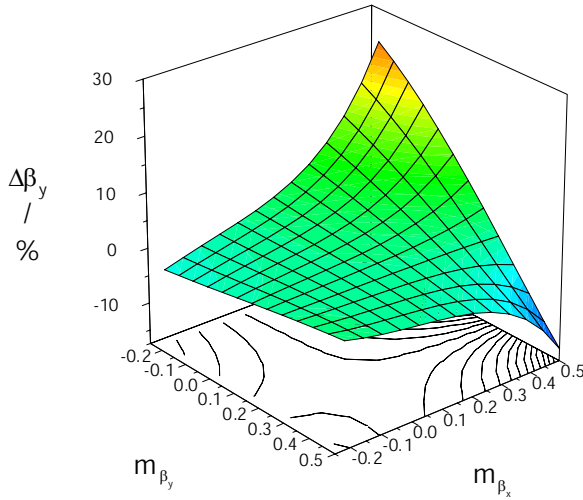

Figure 2: Orthogonality behaviour of the $\beta_x^\star$ knob. $\Delta\beta_y^\star$ is shown as a function of $m_{\beta_x^\star}$ and $m_{\beta_y^\star}$ ($\Delta\beta_y^\star = f(m_{\beta_x^\star}, m_{\beta_y^\star})$). To only see the change of $\beta_y^\star$ created by the $\beta_x^\star$ knob, $\Delta\beta_y^\star$ is normalized as following: $\Delta\beta_y^\star = (\beta_y^\star - \beta_{y_0}^\star)/\beta_{y_0}^\star$, where $\beta_y^\star$ is the actual value and $\beta_{y_0}^\star$ is the value if only the knob vector for $\beta_y^\star$ is applied. The ranges on the x and y axes are $(+100/-50)\%$. Computation was done for version 6.4 using MADX.

The orthogonality behaviour ($\Delta\beta_x^\star = f(m_{\beta_x^\star}, m_{\beta_y^\star})$, $\Delta\beta_y^\star = f(m_{\beta_x^\star}, m_{\beta_y^\star})$) of both knobs is different, where the two variables $m_{\beta_{x,y}^\star}$ denote the knob settings. The reason for this is the antiymmetric lattice as mentioned before. Due to technical and design reasons, the lattice is not strictly asymmetric. Also the phase advance is not anti-symmetric around the IP. All these small differences contribute to the different behaviour of the two planes because a change of the β-function at the IP is related to these variables as follows:

$$\Delta\beta^\star = \frac{\beta^\star}{2\sin(2\pi Q)} \oint \beta(s)\Delta K(s)\cos(2|\Delta\mu| - 2\pi Q)ds.$$
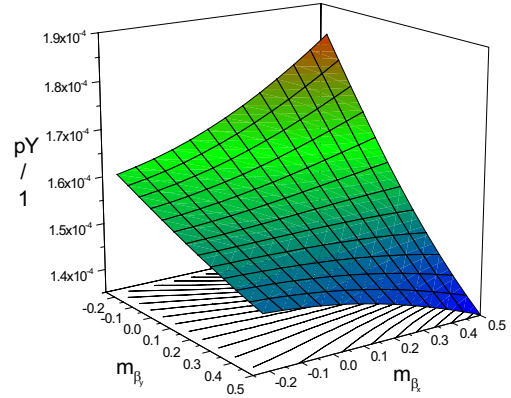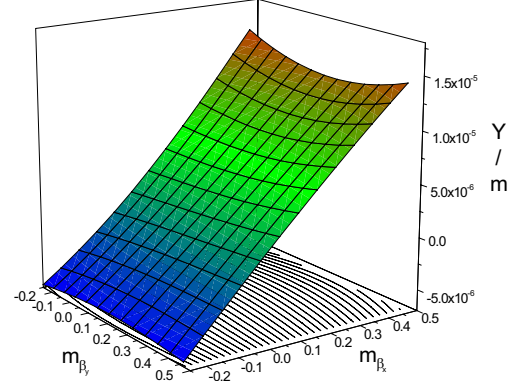

Figure 3: Influence of the knob vectors on Y and the crossing angle pY at IP1. On the x and y axes the values of the scaling factor for the knob m_β for both planes, $m_{\beta_x^\star}$ and $m_{\beta_y^\star}$, are shown within a range of $(+0.5/-0.25)$ with 0.1 units corresponding to 0.1 m. On the z axis the vertical position and slope at the IP, $Y^\star$ and $pY^\star$, are shown. The computation was done for LHC version 6.4 using MADX.

In addition, the dispersion ΔD and β functions have to be monitored around the ring. A change in either of these functions will cause a change at the other IPs which should be avoided. The β function in the x plane does not change around the ring, when the knob is varied, except in the region of IP1, due to the variation of the tuning quadrupoles around IP1. In the plane where the correction is to be applied the beta function through the region between KQ13L and KQ13R is changed to create the needed change of $\beta^\star$. This also introduces changes of β in the other plane with the difference that there $\beta^\star$ is kept constant.

For the dispersion the situation is similar, but different from that without crossing angles. With the vertical crossing angle in IP1 introducing dispersion in the vertical plane dispersion in both planes is to be controlled, even if there is

no cross talk between the planes. So far no critical changes of the dispersion around the ring have been observed.

The changes in the lattice between V6.2 and V6.4 and the new simulation program could be the reason for a slightly degraded behaviour of the knobs. This is being studied.

3   TESTS

To test the behaviour of the knobs, errors were introduced into the lattice. A preliminary correction was applied, i.e., orbit correction for $b1$ field errors, and $b3, b4, b5, a2, a3$ correction with corrector spool pieces, based on magnetic field measuremets. Then the tuning knobs were applied and their effect was observed. To obtain a diversified result, demonstrating for which type of error the knobs work, a test program is followed containing various different types of magnets, fields and errors.

In previous work [5] errors where introduced in the arc dipoles MB and arc quadrupoles MQ. As error field types b1 to b11 were applied. For all cases the $\beta^\star$ values at IP1 could be corrected. Results for errors in all the magnets were summarized in [5]. In these studies no crossing angle was included, and the simulations were performed with lattice version V6.2 and MAD 8.

To test the knobs in the presence of the crossing angle, version V6.4 with MAD X had to be used. Therefore, two test series were performed, one with and one without the crossing angle active. The results are similar in both cases, so that only the results from the test series with active crossing angle is shown in Table 2. The test series were constructed in the same way as in [5] except that no dipole errors were applied for technical reasons.

Table 2: Results from the test run with systematic and random errors of the field error types b2 to b11 in the arc quadrupoles MQ with lattice version V6.4 and MAD X.

	mean value	rms	max neg	max pos		tk appl max pos	tk appl max neg
$\Delta\beta_x^\star$	-1.5E-3	1.23E-2	-3.11E-2	1.88E-2	β_x	5.0E-1	5.0E-1
$\Delta\beta_y^\star$	3.6E-3	1.39E-2	-2.08E-2	3.16E-2	β_y	5.0E-1	5.0E-1
$\Delta D_x^\star$	-8.0E-5	1.41E-3	-4.28E-3	1.99E-3	D_x	2.1E-2	-
$\Delta D_y^\star$	1.9E-5	5.57E-5	-1.06E-4	1.04E-4	D_y	1.0E-2	-
$\Delta Q_1^\star$	64.3115	1.17E-2	-2.25E-2	2.77E-2	Q_1	64.338	64.285
$\Delta Q_2^\star$	59.3215	1.18E-2	-1.82E-2	2.99E-2	Q_2	59.350	59.302
$\Delta X^\star$	2.7E-8	4.73E-7	-7.60E-7	1.42E-6	X	7.0E-8	-4.2E-5
$\Delta Y^\star$	2.6E-8	4.54E-7	-9.27E-7	1.08E-6	Y	2.6E-6	-6.1E-6
$\Delta pX^\star$	-5.9E-8	1.25E-6	-3.68E-6	2.22E-6	pX	7.3E-6	-1.0E-5
$\Delta pY^\star$	1.2E-7	7.41E-7	-1.28E-6	7.18E-5	pY	7.2E-5	-4.8E-7

Columns two and three in Table2 show the mean and rms value of the changes between the introduction of the errors and the application of the tuning knobs, column four the maximum negative, column five the maximum positive change out of sixty different seeds and columns seven and eight the resulting maximum positive and negative final values of $\beta_x^\star, \beta_y^\star, D_x^\star, D_y^\star, Q_x, Q_y, X^\star, Y^\star, pX^\star, pY^\star$ over 60 random seeds after the tuning knobs were applied.

To visualize the correction efficiency the actual correction $\beta_0 + \Delta\beta_c$ is plotted over the to be corrected β_e value. In such a plot, all perfectly corrected seeds lie on the diagonal. This is shown in Fig.4 (left plot) for errors generated in the

arc quadrupoles. The right plot refers to errors generated in the insertion triplet. In the latter case, if the resulting errors in $\beta^\star$ exceed a value of $\approx \pm 25\%$ the knobs fail to work, especially for positive $\Delta\beta$ values.
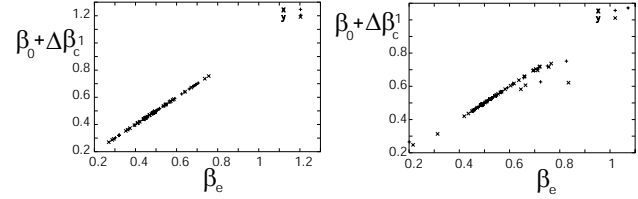

Figure 4: Correction efficiency for errors generated in the arc quadrupoles (left plot) and in the insertion triplet quadrupoles (plot right). The corrected seeds lie on the diagonal. Imperfectly corrected seeds lie off diagonal. The errors of the MQ's were enlarged compared to those expected by a factor of 7. This was done in order to better compare the corresponding correction efficiency with that for errors generated by the insertion triplets.

4   CONCLUSION AND THANKS

So far the characteristics of the calculated tuning knobs are within the given boundaries, except for the changes of the position Y with a maximum of 17% of σ_y for 20% changes in $\beta^\star$. Normal and skew field error types in the arc dipoles and quadrupoles can be corrected with these knobs. The same optics errors generated in the inner triplet quadrupoles cannot be corrected if the $\beta^\star$ change is larger than $\approx 20\%$. This is not too surprising, since triplet errors change the transfer matrices between the knob quadrupoles on either side of the IP. So far the introduction of crossing angles in the lattice shows no major problem except for the induced change in the orbit at the IP. The action of the knobs in the presence of a closed orbit distortion due to field errors in the magnets will be investigated in the future. Finally beam beam effects and the reaction of the knobs to these will complement the picture of the behaviour of the knobs. We thank M. Hayes, O. Bruening and T. Risselada for comments and informations.

5   REFERENCES

[1] H. Grote and F. C. Iselin, 'The MAD program version 8.4: User's reference manual,' CERN-SL-90-13-AP-REV.2.

[2] F. Schmidt, et al., MAD X homepage: http://slap.web.cern.ch/slap/premiereversion.htm

[3] N.J. Walker et al., 'Gloal Tuning Knobs for the SLC Final Focus.' SLAC-PUB-6207,(PAC 93)

[4] Y. Nosochkov, P. Raimondi, T.O. Raubenheimer, A. Seryi, M. Woodley 'Tuning Knobs for the SLC Final Focus.' SLAC-PUB-9255, (EPAC 2002)

[5] W.Wittmer 'Luminosity Optimisation by Adjusting LHC $\beta^\star$ at Collision.' http://icfa-nanobeam.web.ch/icfa-nanobeam/paper/wittmer.pdf